Anomalous Thrust Production from an RF Test Device Measured on a Low-Thrust Torsion Pendulum

David A. Brady[*], Harold G. White[†], Paul March[‡], James T. Lawrence[§], and Frank J. Davies[**]
NASA Lyndon B. Johnson Space Center, Houston, Texas 77058

This paper describes the test campaigns designed to investigate and demonstrate viability of using classical magnetoplasmadynamics to obtain a propulsive momentum transfer via the quantum vacuum virtual plasma. This paper will not address the physics of the quantum vacuum plasma thruster (QVPT), but instead will describe the recent test campaign. In addition, it contains a brief description of the supporting radio frequency (RF) field analysis, lessons learned, and potential applications of the technology to space exploration missions. During the first (Cannae) portion of the campaign, approximately 40 micronewtons of thrust were observed in an RF resonant cavity test article excited at approximately 935 megahertz and 28 watts. During the subsequent (tapered cavity) portion of the campaign, approximately 91 micronewtons of thrust were observed in an RF resonant cavity test article excited at approximately 1933 megahertz and 17 watts. Testing was performed on a low-thrust torsion pendulum that is capable of detecting force at a single-digit micronewton level. Test campaign results indicate that the RF resonant cavity thruster design, which is unique as an electric propulsion device, is producing a force that is not attributable to any classical electromagnetic phenomenon and therefore is potentially demonstrating an interaction with the quantum vacuum virtual plasma.

Nomenclature

α_{power}	=	Specific mass of spacecraft power system, kg/kW$_e$
α_{prop}	=	Specific mass of spacecraft propulsion system, kg/kW$_e$
AU	=	Astronomical Unit (distance from Earth to Sun; ~150M km)
C_3	=	Characteristic energy, km^2/s^2
DDC	=	Dual Directional Coupler
DRO	=	Distant Retrograde Orbit
DUT	=	Device Under Test
kW_e	=	kilowatt, electrical power
LDS	=	Linear Displacement Sensor
LEO	=	Low Earth Orbit
M_{pl}	=	Payload mass
NEP	=	Nuclear Electric Powered
NTR	=	Nuclear Thermal Rocket
PTFE	=	Polytetrafluoroethylene (a.k.a. Teflon)
Q	=	Quality factor
QVPT	=	Quantum Vacuum Plasma Thruster (a.k.a. Q-thruster)
RF	=	Radio Frequency
SEP	=	Solar Electric Powered

[*] Aerospace Engineer, Eagleworks Laboratories, NASA Johnson Space Center (JSC)/EP4, Houston, TX.
[†] Advanced Propulsion Theme Lead and Principal Investigator, Eagleworks Laboratories, NASA Johnson Space Center/EP4, Houston, TX, AIAA Member.
[‡] Principal Engineer, Eagleworks Laboratories, NASA Johnson Space Center/EP4, Houston, TX, AIAA Senior Member.
[§] Electrical Engineer, Eagleworks Laboratories, NASA Johnson Space Center/EP5, Houston, TX.
[**] Electrical Engineer and COMSOL Multiphysics® Analyst, Eagleworks Laboratories, NASA Johnson Space Center/EP5, Houston, TX.

t	=	metric ton (1 t = 1000 kg)
T/m	=	Thrust-to-mass ratio
TExyz	=	Transverse Electric (mode)
TMxyz	=	Transverse Magnetic (mode)
TRL	=	Technology Readiness Level
T_s	=	Thrust-to-power ratio
VCO	=	Voltage Controlled Oscillator
VNA	=	Vector Network Analyzer
VVA	=	Variable Voltage Attenuator

I. Introduction[1]

Much of our current in-space propulsion technology is handicapped by the large propellant mass fraction required by chemical propulsion systems. Interaction with quantum vacuum virtual particles offers the potential to transfer momentum to space vehicles without this propellant mass fraction penalty, similar to the way a naval submarine interacts with the water which surrounds it. Until recently, this interaction has failed to produce sufficient performance to justify aggressive development of the technology. This paper describes our recent efforts to advance the technology readiness level (TRL) of this capability by demonstrating consistent improvements in technology performance, which also demonstrates a steadily-increasing understanding of the analytical and experimental methods needed for successful technology design and operations. This paper closes with a brief illustration of the value proposition associated with applying this technology to space exploration architectures.

Since 2004, researchers at the Northwestern Polytechnical University (NPU) in Xi'an, Shaanxi, China, have been studying microwave-driven resonant cavity thrusters. In 2013, they published a paper[2] that detailed their test campaign results and analysis methodology dealing with a very high powered RF resonant tapered cavity thruster prototype. The thruster was evaluated using an inverted pendulum thrust stand, at a power level from 80 to 2500 watts using two types of magnetrons. The thruster prototype was able to generate thrust magnitudes of over 700,000 micronewtons and had a peak thrust to power performance of ~1 newtons per kilowatt electric (N/kW_e), using raw power numbers for the magnetron. Using the power spectrum for the magnetron provided in their paper, the actual thrust to power was likely much higher as most of the magnetron energy was not absorbed by the RF test article at its target resonant frequency.

During 2013, Eagleworks Laboratories shifted from investigating previous QVPT designs to investigations involving RF resonant cavities. The first portion of the resonant cavity campaign (Cannae) was conducted during the summer of 2013 and was followed by a subsequent campaign (tapered cavity) that commenced in early 2014. Both resonant cavity designs were evaluated using a low-thrust torsion pendulum that is capable of detecting force at a single-digit micronewton level.

II. Thrust Measurement System (Torsion Pendulum)

The Eagleworks Laboratories Low-thrust Propulsion Test Facility at NASA's Johnson Space Center (JSC) is capable of measuring thrust down to the single-digit micronewton level. The central component for this facility is a horizontal torsion pendulum. The torsion pendulum is constructed primarily of aluminum structure that is mounted on a slide-out table within a 30 inch by 36 inch vacuum chamber. The chamber is subsequently mounted on a 4 foot by 8 foot optical bench. The pendulum arm pivots about two linear flexure bearings in a plane normal to gravitational acceleration. The flexure bearings provide an essentially-frictionless and hysteresis-free interface between the static test stand fixed structure and the dynamic pendulum arm. Test article force is measured by measuring the pendulum arm displacement and calculating the force via the flexure bearing spring constants that were determined during test facility setup.

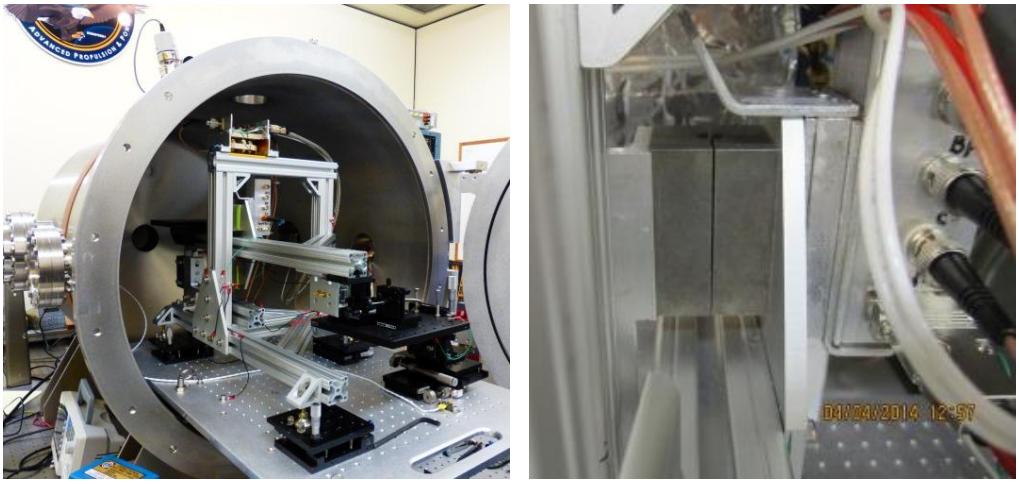

Figure 1. Torsion Pendulum, Vacuum Chamber, and Linear Flexure Bearing

Displacement of the pendulum arm is measured via a Linear Displacement Sensor (LDS). The primary LDS components consist of a combined laser and optical sensor on the fixed structure and a mirror on the pendulum arm. The LDS laser emits a beam which is reflected by the mirror and subsequently detected by the optical sensor. The LDS software calculates the displacement (down to the sub-micrometer level) based upon the beam reflection time. Prior to a test run data take, the LDS is positioned to a known displacement datum (usually 500 micrometers) via mechanical adjustments to its mounting platform. Gross adjustments are performed via set screws. Fine adjustments are performed using manually-operated calibrated screw mechanisms and a remotely controlled motorized mechanism that can be operated with the chamber door closed and the chamber at vacuum. The remote adjustment capability is necessary since the LDS datum will change whenever a change to the test facility environment affects the roll-out table or the chamber – e.g., whenever the chamber door is closed or latched and whenever the chamber is evacuated. Once the LDS displacement is adjusted in the final test environment, further adjustment between test run data takes is usually not required.

Figure 2. Linear Displacement Sensor (LDS) and Adjustment Remote Control

Immediately prior to a test run data take, the displacement/force relationship is verified by inducing a known force onto the pendulum arm and measuring the displacement. This is done via the electrostatic fins calibration mechanism. This mechanism uses two sets of aluminum fins, one set on the fixed structure and one set on the pendulum arm. The fins overlap without touching. A calibration voltage is applied to the fixed structure fins, which induces a force upon the pendulum arm fins and an associated displacement that is measured by the LDS. The electrostatic fins design provides a constant force over a reasonably large range (between 30-70% overlap), so adjustments to the calibration mechanism between test run data takes and even between test article reconfiguration are usually not required. Calibration of the overlap/force relationship was accomplished using a Scientech SA 210 precision weighing balance (resolution to one micronewton).

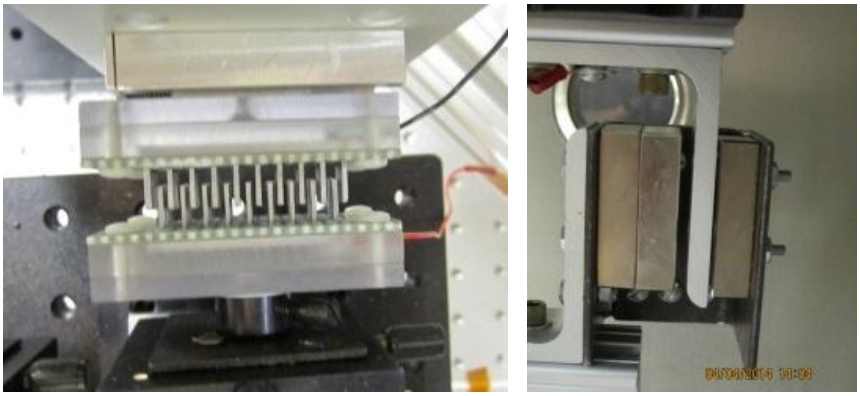

Figure 3. Electrostatic Fins Calibration System and Magnetic Damper

Whenever a force is induced upon the pendulum arm, the resultant harmonic motion must be damped. This is accomplished via the use of a magnetic dampening system (MDS) at the back of the test rig. Three Neodymium (NdFeB Grade N42) block magnets interact with the pendulum's aluminum angle to dampen oscillatory motion.

To simulate the space pressure environment, the test rig is rolled into the test chamber. After sealing the chamber, the test facility vacuum pumps are used to reduce the environmental pressure down as far as 5x10E-6 Torr. Two roughing pumps provide the vacuum required to lower the environment to approximately 10 Torr in less than 30 minutes. Then, two high-speed turbo pumps are used to complete the evacuation to 5x10E-6 Torr, which requires a few additional days. During this final evacuation, a large strip heater (mounted around most of the circumference of the cylindrical chamber) is used to heat the chamber interior sufficiently to emancipate volatile substances that typically coat the chamber interior walls whenever the chamber is at ambient pressure with the chamber door open. During test run data takes at vacuum, the turbo pumps continue to run to maintain the hard vacuum environment. The high-frequency vibrations from the turbo pump have no noticeable effect on the testing seismic environment.

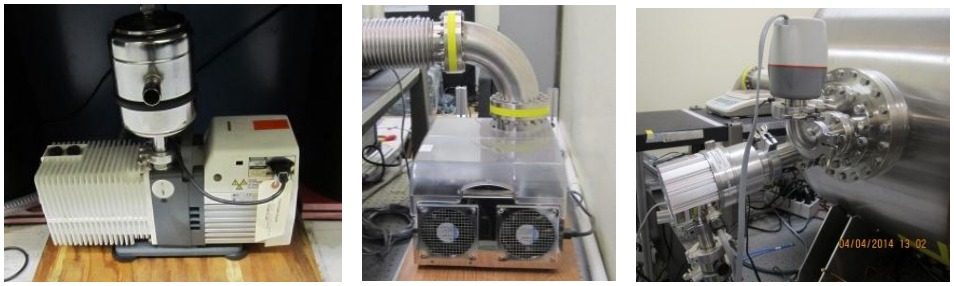

Figure 4. Vacuum Pumps (two roughing pumps and two turbopumps)

However, one visible affect to the seismic environment is the periodic (about one-third to one-quarter Hertz) perturbation created by the waves from the Gulf of Mexico (about 25 miles southeast of Johnson Space Center), especially on windy days. According to local geologists, these low frequency waves propagate inland as far as 100 miles. A less predictable and higher impact seismic disturbance is the equipment and activity in the areas adjacent to the Eagleworks Lab test area, including a building air handler, an elevator, and employee foot traffic. In order to minimize impacts of all vibration sources, the table is floated on its pneumatic vibration isolation piers.

Figure 5. Vacuum Chamber with Mounted Strip Heater & Rack-mounted Data Acquisition System

Additional equipment for power, signal generation, and data collection and display resides in the lab equipment rack adjacent to the optical bench. From this location, our Test Engineer can provide test article primary power, RF signal generation, signal amplification, avionics control power, data acquisition, and data display.

All power and signals pass between the external equipment and vacuum chamber internal components via sealed feedthrough ports. Inside the vacuum chamber, all power and signals that pass between the torsion pendulum fixed structure and the pendulum arm are transmitted via liquid metal contacts in order to eliminate interface cable forces. Each liquid metal contact consists of a physical but non-force-producing interface between a brass screw and a small socket filled with Galinstan™ liquid metal (a commercially available alloy consisting mainly of gallium, indium, and tin). Galinstan™ has a low toxicity and reactivity, so it is often used in place of mercury.

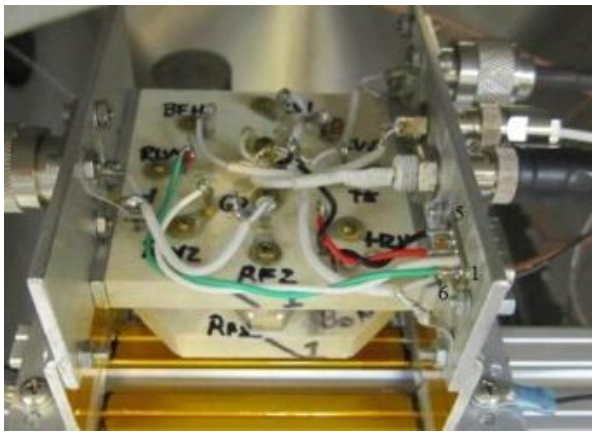

Figure 6. Liquid Metal Contacts

The propulsion test article is mounted on the end of the pendulum arm closest to the chamber door. Test article support electronics – e.g., signal generators, amplifiers, phase adjusters - may be mounted on either end of the pendulum arm. If needed, ballast is added to the pendulum arm to eliminate moments that affect the neutral position of the pendulum arm.

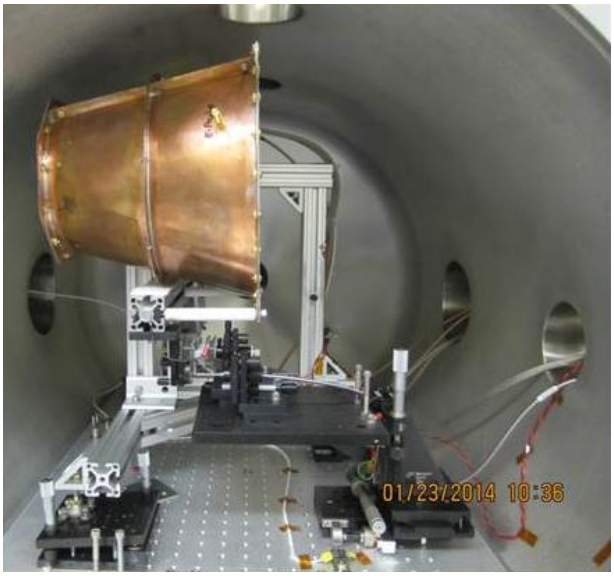

Figure 7. Tapered Cavity Test Article Mounted on Torsion Pendulum

After a test article is mounted on the pendulum arm, a typical test run data take consists of a pre-run calibration (using the electrostatic fin mechanism), followed by energizing the test article (and sometimes manually tuning the frequency), and finishing with a post-run calibration and data recording.

III. Cannae Test Campaign

A. Description of Test Elements and Test Setup

The Cannae test article is a pillbox/beam pipe design fashioned after an RF resonant cavity design used in high energy particle accelerators. Each Cannae test article is approximately 11 inches in diameter and 4-5 inches between the ends of the beam pipes, not counting beam pipe extensions or antenna mounts. Cannae modified the particle accelerator design by engraving radial slots (1.4 inches long by 0.4 inches wide by 0.4 inches deep) along the outside edge of the resonant cavity interior, but on only one side of the pillbox (equatorially-asymmetric).[3]

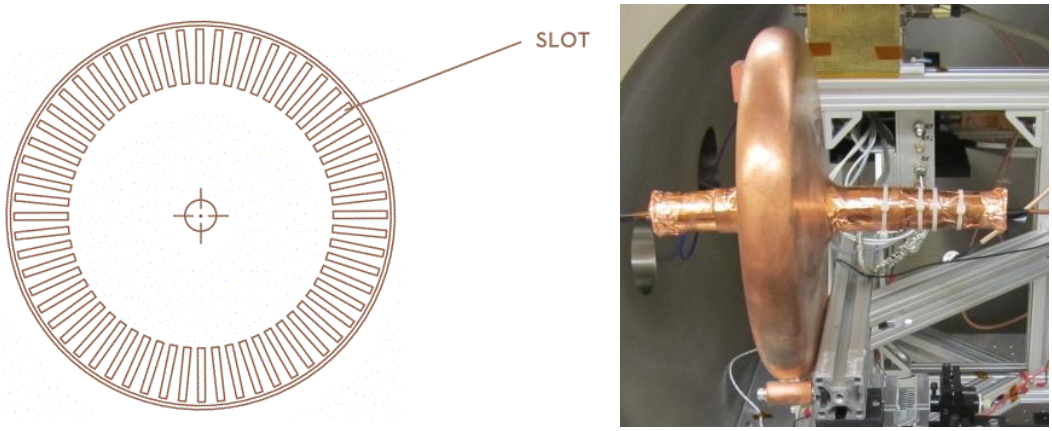

Figure 8. Slotted Pillbox Cavity (view down beam pipe central axis) and Test Article Close-up

Prior to testing, Cannae theorized that the asymmetric engraved slots would result in a force imbalance (thrust). As a result, a second (control) test article was fabricated without the internal slotting (a.k.a. the null test article). In addition, both test articles (slotted and unslotted) were tested in both the forward thrust and the reverse thrust (beam

pipe central axis rotated 180 degrees) orientation. An amplified RF signal is fed into one of the test article beam pipes via an approximately 20-gauge copper wire drive antenna. On the opposite beam pipe, an approximately 20-gauge copper wire serves as a sense antenna that provides the cavity RF signal frequency so the Test Engineer can manually adjust the RF frequency input to maintain the cavity resonant frequency during a test run. Cavity resonant frequency is determined during a pre-test cavity evaluation using a vector network analyzer (VNA). In addition, beam pipe extensions were added and held in place by adhesive copper tape, electrical tape, and nylon tie wraps as needed to position the drive and sense antennas, in order to manage (or measure) the electric and magnetic fields in the beam pipe and the pillbox. Figure 9 shows a test article mounted on the torsion pendulum during a test campaign, and a test block diagram follows. The longer beam pipe is the RF drive antenna that in practice ends up being a ¼ wave resonance system in its own right and has a dielectric PTFE slug in the throat in both the slotted and null test article. It is this characteristic that became an item of further consideration after completion of the test campaign.

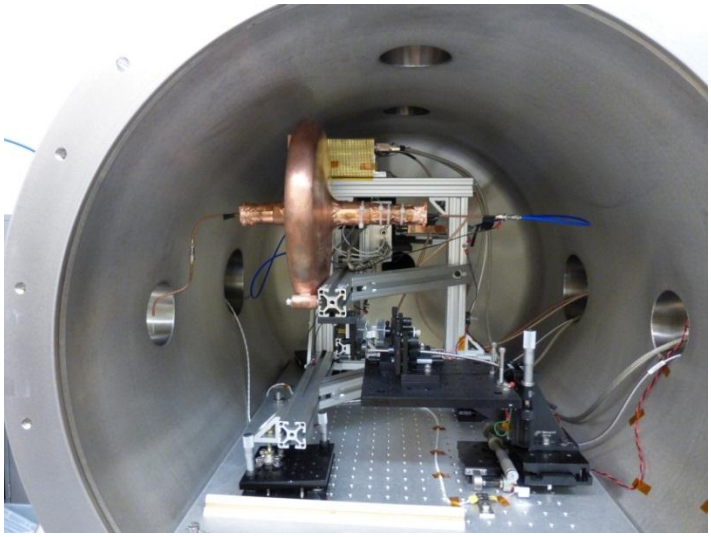

Figure 9. Cannae Test Article on Torsion Pendulum (thrust to the left, a.k.a. forward orientation)

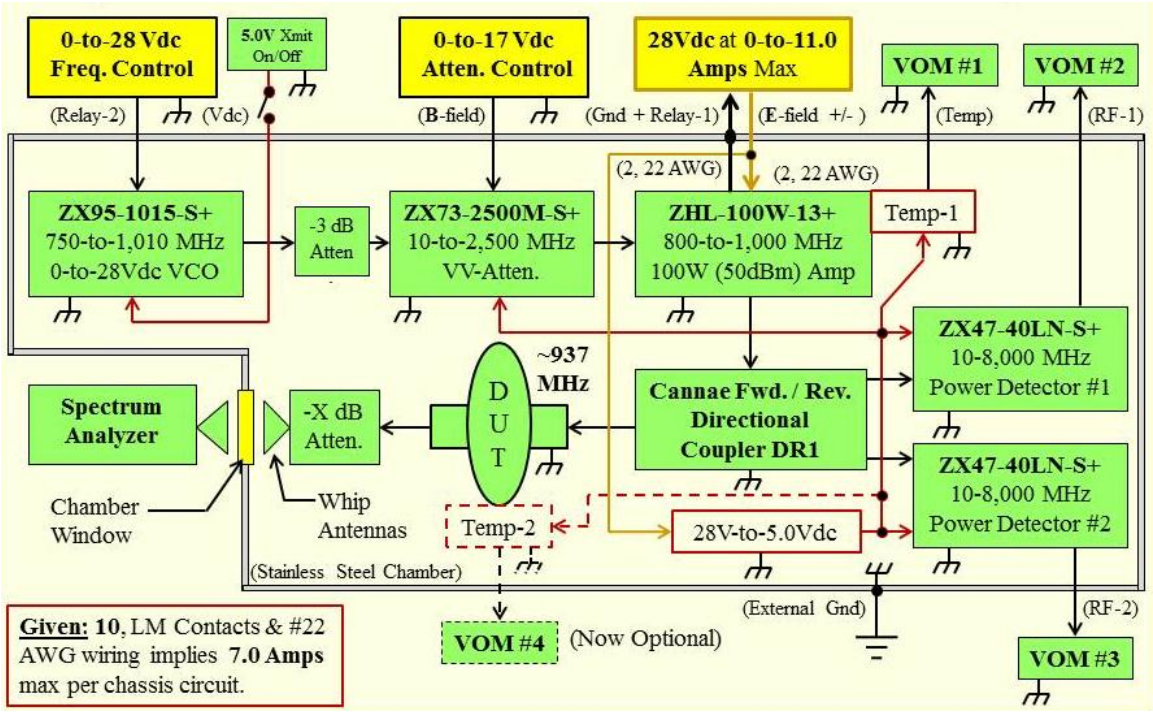

Figure 10. Block Diagram of Cannae Test Setup.
The 100 W amplifier was replaced with a 30 W amplifier during pre-test integration.

During testing, the Test Engineer controls the RF frequency generation via a 0-to-28 volts dc power input to a voltage-controlled oscillator (VCO). The VCO RF signal output is passed to a variable voltage attenuator (VVA), the output of which is controlled by the Test Engineer via a 0-to-17 volts dc power input. Based upon the VVA output, the amplifier will output up to approximately 28 watts. Amplifier output passes to a dual-directional coupler (DDC), which allows forward and reflected power measurements to be obtained as the power is simultaneously passed to the test article input port. The Test Engineer monitors forward and reflected power and adjusts the input frequency to obtain the desired combination of cavity frequency and power delivery to the cavity.

B. Cannae Slotted Cavity (Test Article #1) Testing

Testing was performed in two orientations, one to test for thrust in one direction (Test Configuration 1A) and an opposing orientation (beam pipe central axis rotated 180 degrees) to test for thrust in the opposite direction (Test Configuration 1B). Figure 11 shows the Cannae test article mounted so that the thrust is directed to the right of the picture.

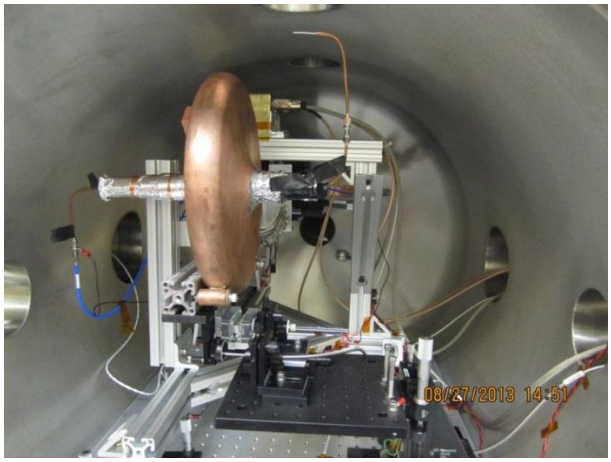

Figure 11. Cannae Test Article on Torsion Pendulum (thrust to the right, a.k.a. reverse orientation)

During Test Configuration 1A, the Test Article #1 (slotted) cavity was energized five times at an amplifier output power of approximately 28 watts and at a frequency of approximately 935 MHz, resulting in pendulum arm displacements that corresponded to test article thrust between 31.7 and 45.3 (40.0 mean) micronewtons. Torsion pendulum calibration displacements (corresponding to approximately 29 micronewtons each) were performed immediately before and after each thrust measurements. Figure 12 represents a typical data run.

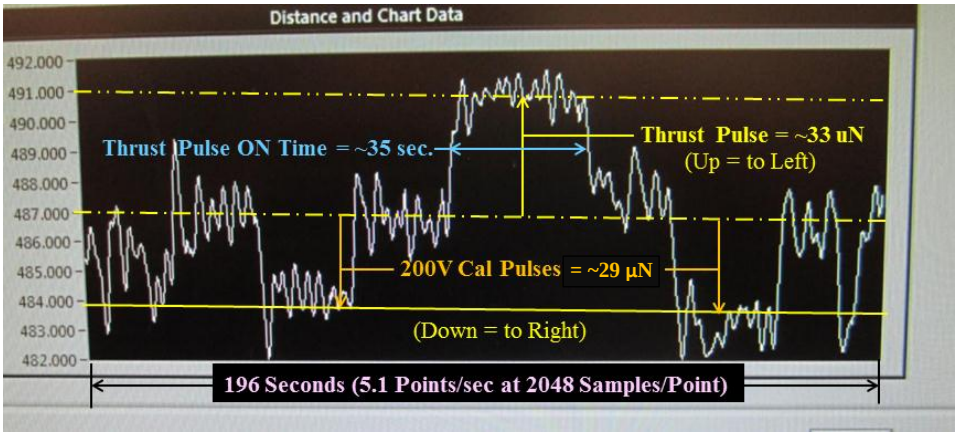

Figure 12. Representative Test Run (Configuration 1A)

During Test Configuration 1B, the Test Article #1 (slotted) cavity was energized only once (due to test schedule constraints) at an amplifier output power of approximately 28 watts and at a frequency of approximately 936 MHz, resulting in a pendulum arm displacement that corresponded to test article thrust of approximately 48.5 micronewtons. Torsion pendulum calibration displacements (corresponding to approximately 29 micronewtons each) were performed immediately before and after thrust measurements.

C. Cannae Unslotted Cavity (Test Article #2) Testing

Testing was performed in two orientations, one to test for thrust in one direction (Test Configuration 2A) and an opposing orientation (beam pipe central axis rotated 180 degrees) to test for thrust in the opposite direction (Test Configuration 2B).

During Test Configuration 2A, the Test Article #2 (unslotted) cavity was energized four times at an amplifier output power of approximately 28 watts and at a frequency of approximately 932 megahertz, resulting in pendulum arm displacements that corresponded to test article thrust between 35.3 and 50.1 (40.7 mean) micronewtons.

Torsion pendulum calibration displacements (corresponding to approximately 29 micronewtons each) were performed immediately before and after thrust measurements.

During Test Configuration 2B, the Test Article #2 (unslotted) cavity was energized only once (due to test schedule constraints) at an amplifier output power of approximately 28 watts, resulting in pendulum arm displacements that corresponded to test article thrust of 22.5 micronewtons. Torsion pendulum calibration displacements (corresponding to approximately 29 micronewtons each) were performed immediately before and after thrust measurements.

D. Systemic Effect Evaluation (using RF Load)

Finally, a 50 ohm RF resistive load was used in place of the test article to verify no significant systemic effects that would cause apparent or real torsion pendulum displacements. The RF load was energized twice at an amplifier output power of approximately 28 watts and no significant pendulum arm displacements were observed. Torsion pendulum calibration displacements (corresponding to approximately 29 micronewtons each) were performed immediately before and after thrust measurements.

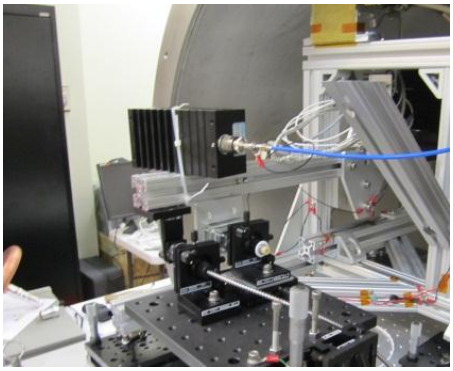

Figure 13. RF Resistive Load mounted on torsion pendulum

E. COMSOL Multiphysics® Analysis of Cannae Cavities

Computer modeling of the electric field within the pillbox and beam pipe (using COMSOL Multiphysics® software, hereafter referred to as "COMSOL®") illustrates the relative weakness of the electric field in the vicinity of the cavity slots and relative strength of the electric field within the beam pipe, especially in the drive antenna coaxial cable and the region around the cable within the PFTE dielectric slug as seen in Fig. 14. Consideration of the dynamic fields in the ¼ wave resonance tube shows that there is always a net Poynting vector meaning that the RF launcher tube assembly with dielectric cylinder common to both the slotted and smooth test articles is potentially a Q-thruster where the pillbox is simply a matching network.

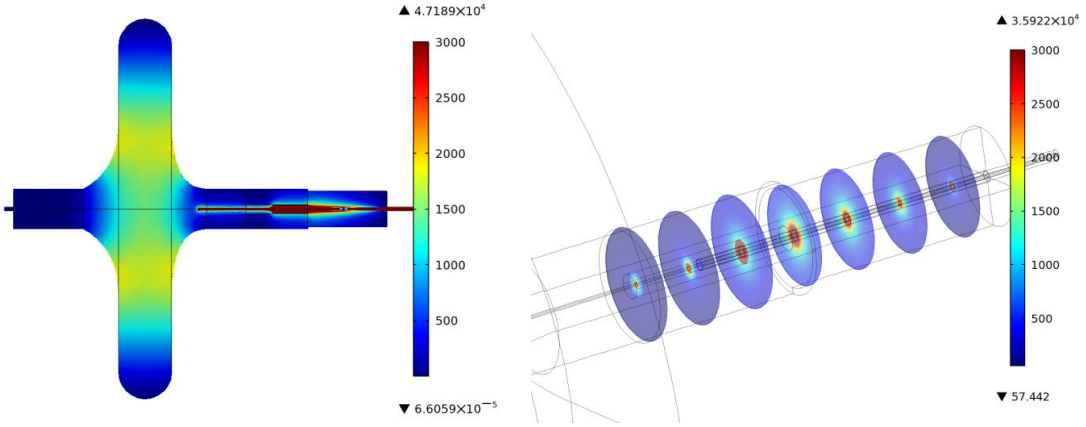

Figure 14. Cross section of test article (left) and close up of fields in RF drive pipe (right)

F. Cannae Testing: Lessons Learned during Integration and Testing

Almost six days were required from equipment delivery to first thrust measurement for test preparation and integration activities. The most significant challenge was RF system engineering, including manual frequency control of the RF test article. Lessons learned included:

- At ~1 GHz frequencies, RF signal leakage can be substantial if all interfaces are not properly RF shielded. All cables, components, and connectors must be designed or sealed (e.g., with conductive tape or a Faraday cage) to eliminate (or at least reduce) RF leak paths. Be aware of the circuit protection specifications on RF amplifiers.

- Manual control of the resonant cavity frequency will add a substantial amount of time to the test schedule. Eagleworks implemented an automated, phase-locked loop (PLL) frequency control circuit during a subsequent test campaign.

- Cable routing must be evaluated and designed to prevent ground loops. This was a not a significant challenge during this campaign, but it became more difficult after implementation of the PLL during a subsequent test campaign.

G. Cannae Testing: Summary of Results and Conclusions

Configuration	Test Article	Thrust Direction	Thrust Range (μN)	Mean Thrust (μN)	Number of Test Runs
1A	Slotted	Forward	31.7 – 45.3	40.0	5
1B	Slotted	Reverse	48.5	48.5	1
2A	Unslotted	Forward	35.3 – 50.1	40.7	4
2B	Unslotted	Reverse	22.5	22.5	1
RF Load	50Ω Load	N/A	0.0	0.0	2

Table 1. Cannae Testing: Summary of Results and Conclusions

The resistive RF Load evaluation indicated no significant systemic cause for torsion pendulum displacement. Based upon this observation, both test articles (slotted and unslotted) produced significant thrust in both orientations (forward and reverse). Test schedule constraints prevented multiple data points to be gathered in the reverse orientation, and the single data point for each test article is insufficient to allow comparative conclusions (between slotted and unslotted) to be drawn. However, for the forward thrust orientation, the difference in mean thrust between the slotted and unslotted was less than two percent. Thrust production was not dependent upon the slotting.

IV. Tapered Cavity Test Campaign

A. Tapered Cavity RF Evaluation, General

Figure 15 depicts one of the early COMSOL® models representing an early possible construction of a tapered RF unit alongside the actual construction that was finally implemented as informed by COMSOL® analysis. The RF drive antenna is the lower loop antenna seen in the wireframe representation of the assembly. An S11 (reflected power) plot prediction from COMSOL® is evaluated against the actual S11 output as measured by a vector network analyzer (VNA) connected to the lower antenna. Note that, in practice, a second (RF sense) antenna is present in the thruster in anticipation of implementing a phase lock loop (PLL) control approach to maintain resonance conditions over time. With the presence of the second RF sense antenna, COMSOL® can be used to provide an S21 (two-port

delivered power) plot prediction that can also be evaluated against the actual S21 plot from a VNA connected to both the drive and sense antenna. Comparing the S11 and S21 predicted plots with actual plots helps ensure that the RF drive system is properly coupling with the desired electromagnetic mode at a particular frequency.

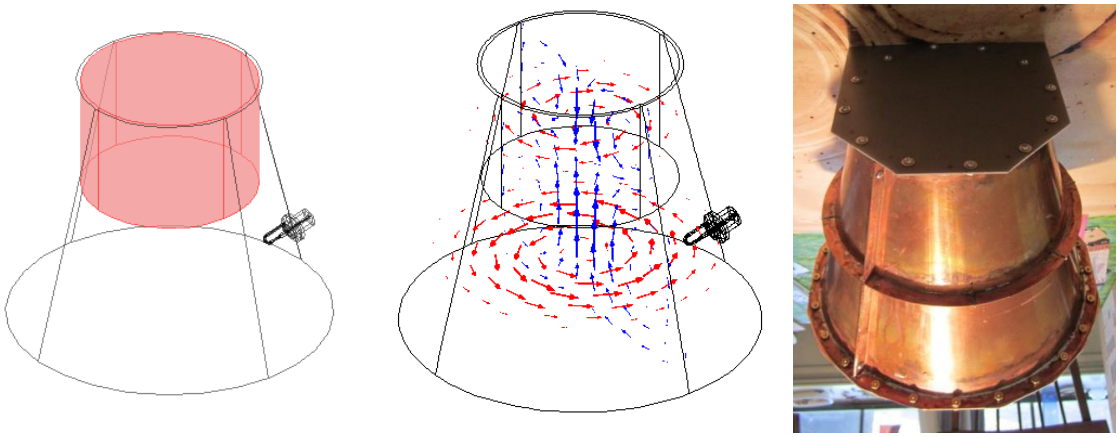

Figure 15. COMSOL® Tapered RF model, TE012 results, and early construction

The COMSOL analysis iteration process was used prior to assembly to determine the optimal thickness and diameter of the dielectric RF resonator disc located at the small end of the thruster. The geometry of the RF resonator disc is a function of the resonator material's relative permittivity, dissipation factor, and target resonance mode.

The first step in performing a test evaluation run with the tapered thruster is to identify the modes of interest using the predicted S11 and S21 plots as compared to observation. Figure 16 depicts the COMSOL prediction and what was observed.

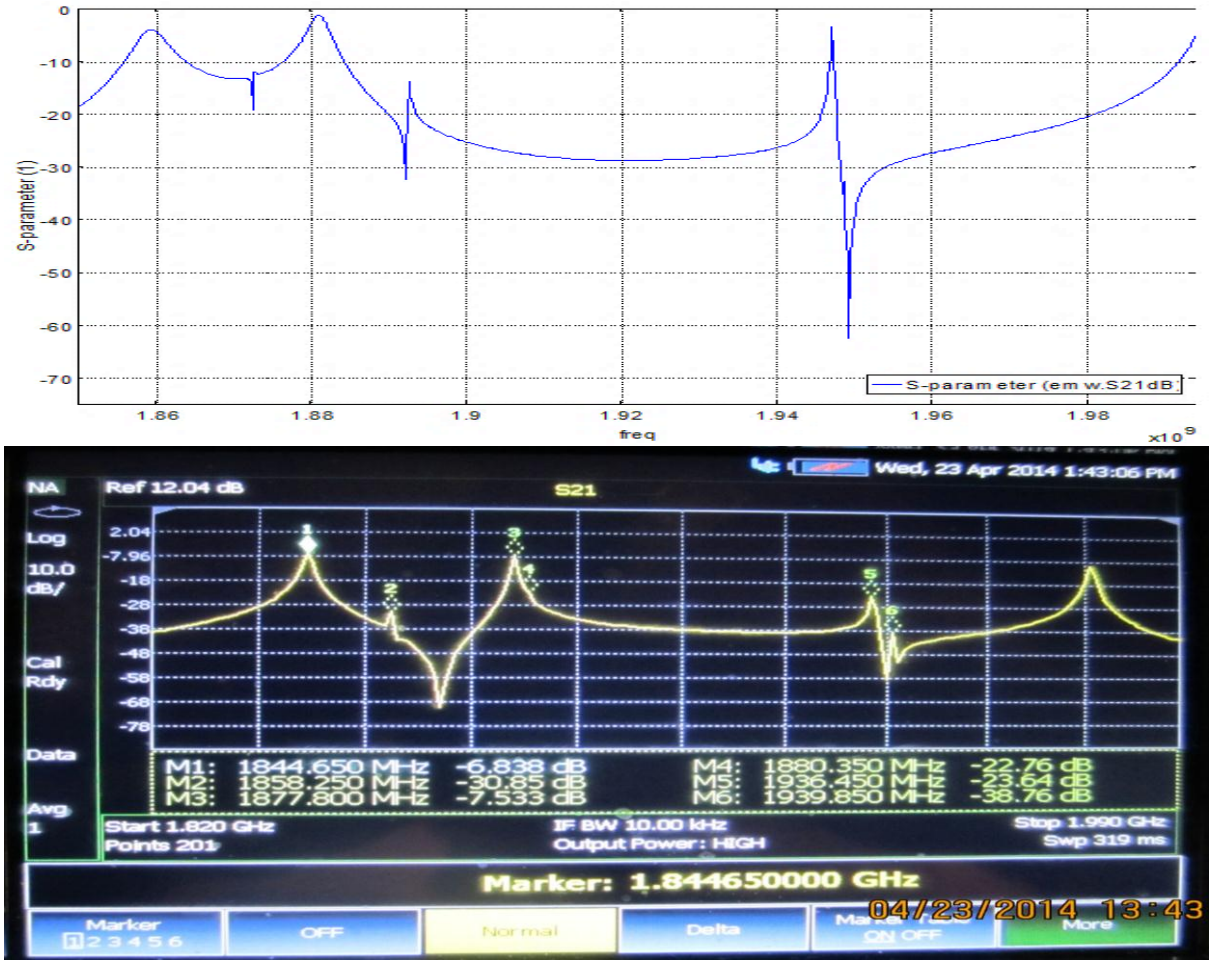

Figure 16. Predicted and Actual S21 plots

Testing of the tapered RF thruster at a particular mode started with some bench level evaluation of the choice of RF drive antenna (type, size, and mounting orientation), and likewise for the sense antenna. When this step was complete, the thruster was transferred to the low thrust torsion pendulum and connected to the manually tuned RF drive system (which simultaneously served as the counterbalance mass for the thruster at the opposite end of the torsion pendulum arm). The 25 watt amplifier was driven by a Mini-Circuits® voltage controlled oscillator (VCO) passed through a Mini-Circuits® variable voltage attenuator (VVA). The output of the RF amplifier was run through a dual directional coupler (DDC) with power meters positioned to measure forward and reflected power from the test article. For final tuning prior to testing on the rig, typically a stub tuner was placed between the DDC and the test article and the VNA's Smith Chart and S11 plots were used to optimize coupling with the test article. Figure 17 shows the thruster mounted on the torsion pendulum arm and how it was connected to the RF amplifier.

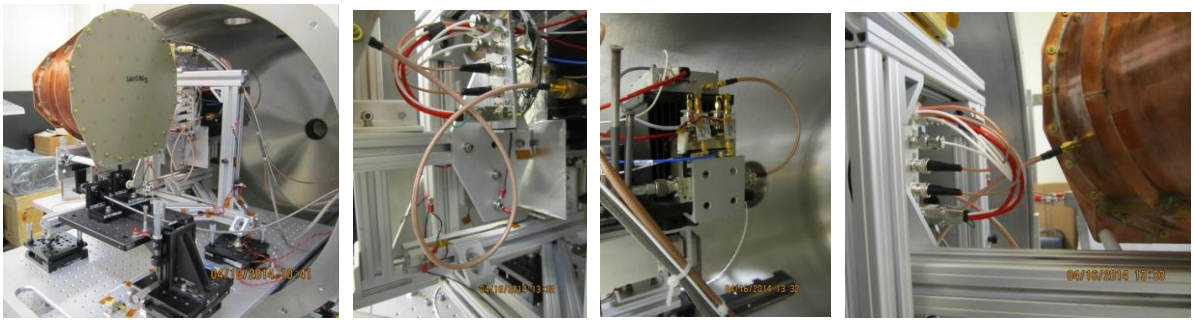

Figure 17. Typical Tapered Cavity RF Thruster Test Configuration (left to right): thruster on torsion pendulum; 2' RG-142 shielded cable to RF thruster; 1' RG-142 shielded cable from amplifier to dual directional coupler (stub tuner and power meters can be seen); 2' RG-142 cable connected to thruster 16mm loop antenna

B. Tapered Cavity RF Evaluation and Testing, First TM211 mode

Figures 18 and 19 chronicle the activities surrounding a series of five test runs at 1932.6 MHz corresponding to the first TM211 mode. In this test configuration, the VNA system indicated a quality factor of ~7320, and the difference of power forward and power reflected as reported by the power meters was indicated to be ~16.92 watts as a result of manual tuning to maximize the power difference. The (net) peak thrust observed for this tested configuration was 116 micronewtons and the (net) mean thrust over the five runs was 91.2 micronewtons. The net force is calculated by accounting for the null force present in the system. Null testing is performed by attaching the RF drive system to a 50 ohm load and running the system at full power. The null force testing indicated that there was an average null force of 9.6 micronewtons present in the as tested configuration. The presence of this null force was a result of the DC power current of 5.6 amps running in the power cable to the RF amplifier from the liquid metal contacts. This current causes the power cable to generate a magnetic field that interacts with the torsion pendulum magnetic damper system. The null test data is also shown in Fig. 20.

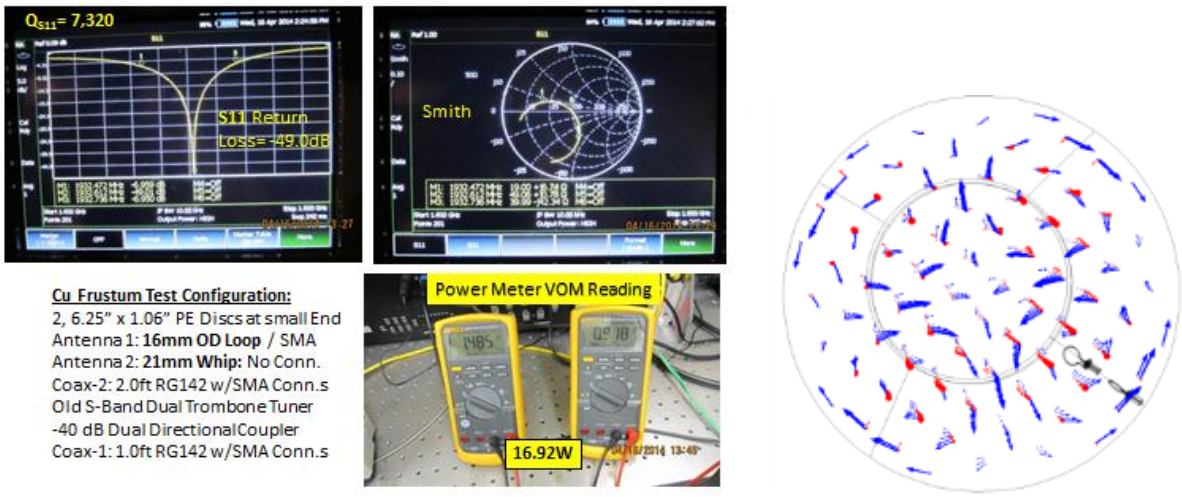

Figure 18. VNA S11 return loss plot, Smith plot, and power meter readings for 1932.6 MHz, TM211 mode (COMSOL® field plot also shown for reference - red is electric, blue is magnetic)

Figure 19. Five thrust pulses of tapered RF system at 1932.6 MHz, peak thrust performance of 116 micronewtons, average thrust performance of 91.2 micronewtons

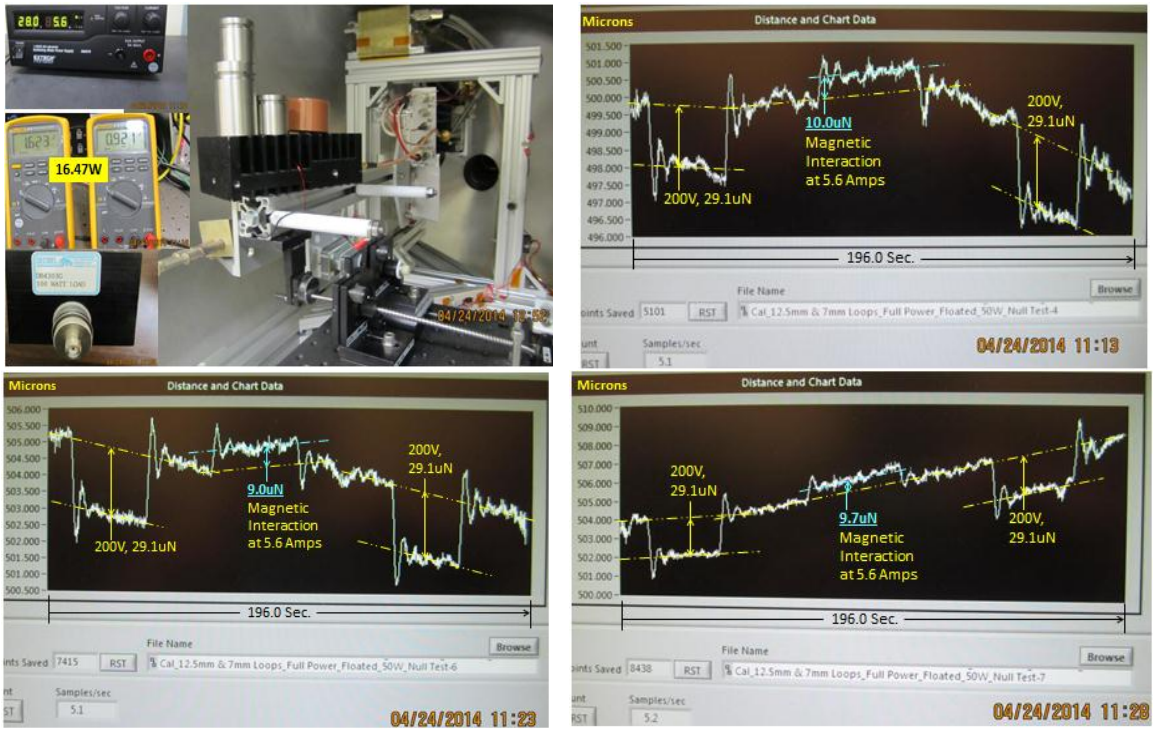

Figure 20. Null Test on Torsion Pendulum – average null force is 9.6 micronewtons due to 5.6A DC current in power cable (routes power from liquid metal contacts to RF amplifier; interacts with magnetic damper system)

The COMSOL analysis for the first TM211 mode had a predicted quality factor of 7961 and a thrust to power performance magnitude of 20 micronewtons per watt. With an input power of 17 watts, correcting for quality factor, the predicted thrust is 313 micronewtons.

C. Tapered Cavity RF Evaluation and Testing, Second TM211 mode

COMSOL® analysis indicates that there are two TM211 modes within a couple of MHz of one another for the as-built tapered thruster. The higher frequency TM211 mode has a much higher predicted quality factor (32,125), but considerably lower thrust to power performance (5 micronewtons per watt). The tapered RF system was tuned and operated at this mode for evaluation on the low thrust torsion pendulum. The measured quality factor was 18,100 with a power-forward/power-reflected difference of 16.74 watts and the average measured thrust was 50.1 micronewtons. With an input power of 16.74 watts, correcting for the quality factor, the predicted thrust was 47 micronewtons. It should be noted that the drive antenna was changed to a 12.5mm circular loop antenna, and the stub tuner was removed and the orientation of the loop antenna was used for tuning prior to testing. Figure 21 shows the as-tuned conditions tested.

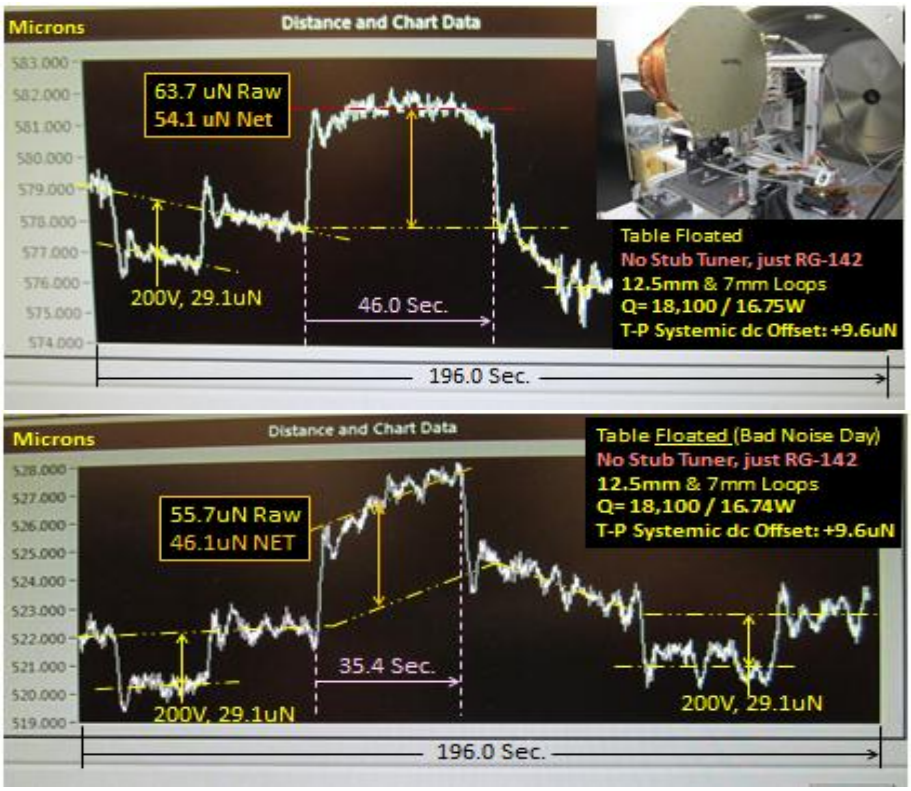

Figure 21. Two thrust pulses of tapered RF system at 1936.7 MHz, peak thrust performance of 54.1 micronewtons, average thrust performance of 50.1 micronewtons

D. Tapered Cavity RF Evaluation and Testing, TE012 mode

Prior to the TM211 evaluations, COMSOL® analysis indicated that the TE012 was an effective thrust generation mode for the tapered cavity thruster being evaluated, so this mode was explored early in the evaluation process. Figure 22 shows a test run at the TE012 mode with an operating frequency of 1880.4 MHz. The measured quality factor was ~22,000, with a COMSOL prediction of 21,817. The measured power applied to the test article was measured to be 2.6 watts, and the (net) measured thrust was 55.4 micronewtons. With an input power of 2.6 watts, correcting for the quality factor, the predicted thrust is 50 micronewtons. However, since the TE012 mode had numerous other RF modes in very close proximity, it was impractical to repeatedly operate the system in this mode, so the decision was made to evaluate the TM211 modes instead.

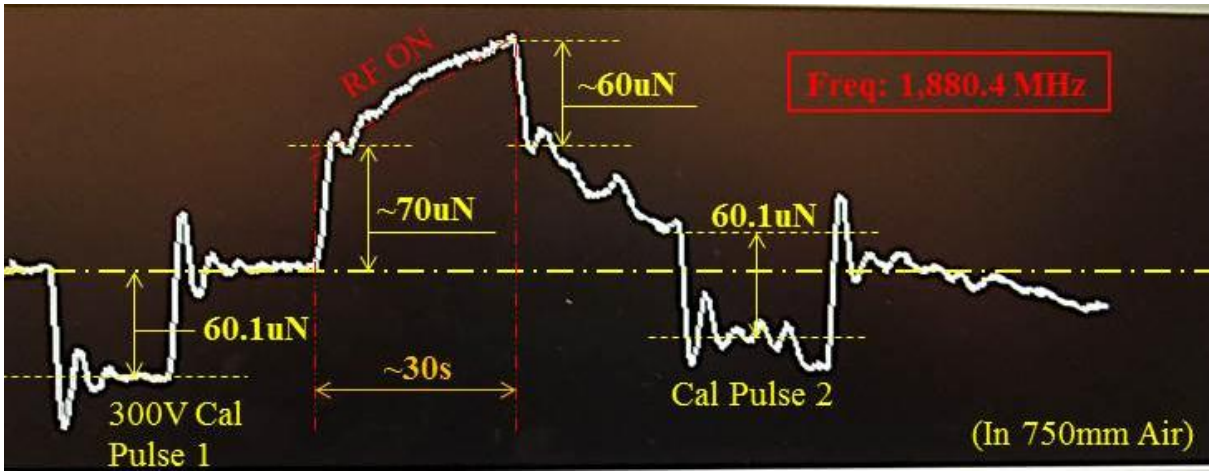

Figure 22. TE012 test data, quality factor of 22000, applied power of 2.6 watts, net average thrust of 55.4 micronewtons

E. Tapered Cavity Testing: Summary of Results

Mode	Frequency (MHz)	Quality Factor, Q	Input Power (W)	Peak Thrust (μN)	Mean Thrust (μN)	Number of Test Runs
TM211	1932.6	7320	16.9	116.0	91.2	5
TM211	1936.7	18,100	16.7	54.1	50.1	2
TE012	1880.4	22,000	2.6	55.4	55.4	1

Table 2. Tapered Cavity Testing: Summary of Results

F. Tapered Cavity RF Evaluation, General Findings and Lessons Learned

Overall, the biggest lesson learned was that RF tuning and optimization constraints are very challenging. We discovered early in the COMSOL® analysis process that just because you can achieve a great RF solution does not mean that it will be an ideal Q-thruster implementation.

There appears to be a clear dependency between thrust magnitude and the presence of some sort of dielectric RF resonator in the thrust chamber. The geometry, location, and material properties of this resonator must be evaluated using numerous COMSOL® iterations to arrive at a viable thruster solution. We performed some very early evaluations without the dielectric resonator (TE012 mode at 2168 MHz, with power levels up to ~30 watts) and measured no significant net thrust.

Numerous COMSOL® analysis runs also indicated a strong dependency between thrust magnitude and antenna type, location, orientation, and number of antenna feeds. Slight changes in antenna design and number of feeds changed the COMSOL® thrust prediction by a factor of three which forced our team to implement tighter configuration control protocols during testing to ensure close representation of as built hardware to the analyzed configuration.

Finally, our experience with the TE012 mode indicated that it is important to design the RF prototype such that any target mode of operation is as isolated as possible in the frequency domain to help ensure that the system can be effectively tuned manually. This also protects for the ability to implement and use a phase lock loop (PLL)

automated frequency control circuit. Due to the slow process commensurate with manual tuning, our future test articles will make use of a PLL whenever practical in order to increase the amount of data that can be collected for a given test article configuration and operating condition during a given amount of test time.

V. Application of Technology to Space Exploration Missions

Based on test data and theoretical model development, the expected thrust to power for initial flight applications is expected to be in the 0.4 newton per kilowatt electric (N/kW_e) range, which is about seven times higher than the current state of the art Hall thruster in use on orbit today. The following figures show the value proposition for this class of electric propulsion. Figure 23 shows a conservative 300 kilowatt solar electric propulsion roundtrip human exploration class mission to Mars/Deimos. Figure 24 shows a 90 metric ton 2 megawatt (MW) nuclear electric propulsion mission to Mars that has considerable reduction in transit times due to having a thrust to mass ratio greater than the gravitational acceleration of the Sun (0.6 milli-g's at 1 AU). Figure 25 shows the same spacecraft mass performing a roundtrip mission to the Saturn system spending over a year around two moons of interest, Titan and Enceladus. Even in this last class of mission which requires only a single heavy lift launch vehicle, the mission has less mission duration than is common with a current conjunction-class Mars mission using chemical propulsion systems and which would require multiple heavy lift launch vehicles.

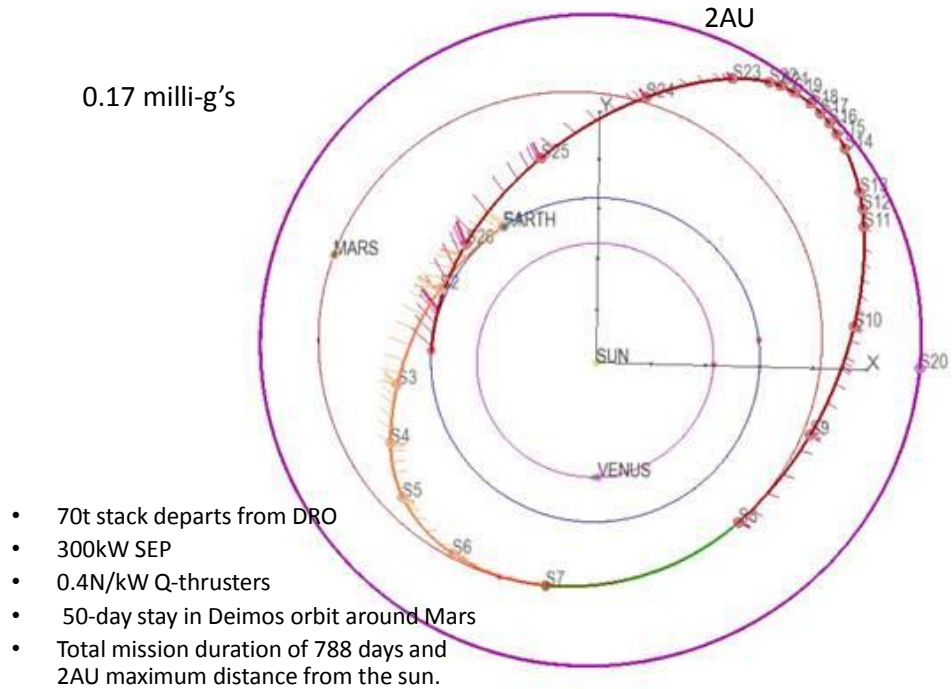

- 70t stack departs from DRO
- 300kW SEP
- 0.4N/kW Q-thrusters
- 50-day stay in Deimos orbit around Mars
- Total mission duration of 788 days and 2AU maximum distance from the sun.

Figure 23. 300 kW SEP Roundtrip Mission to Mars Deimos (50 day stay) departing from DRO

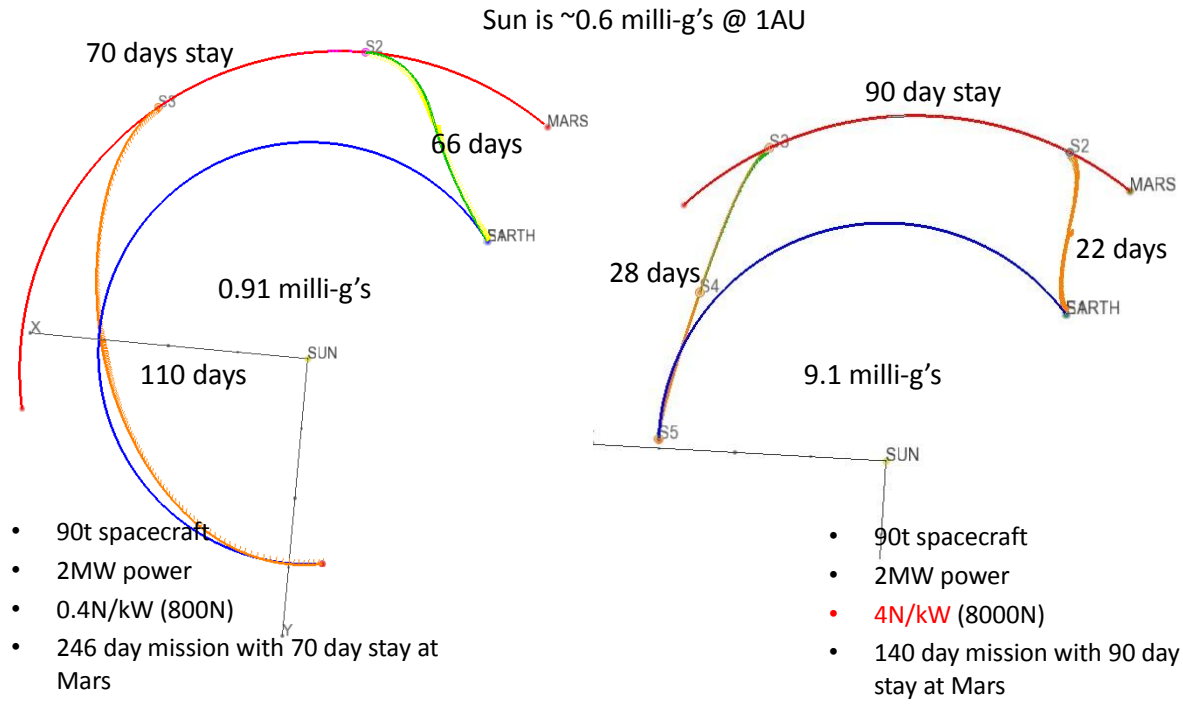

Figure 24. 2MW NEP Roundtrip Mission to Mars with 0.4N/kW$_e$ and 4.0 N/kW$_e$ thrust to power

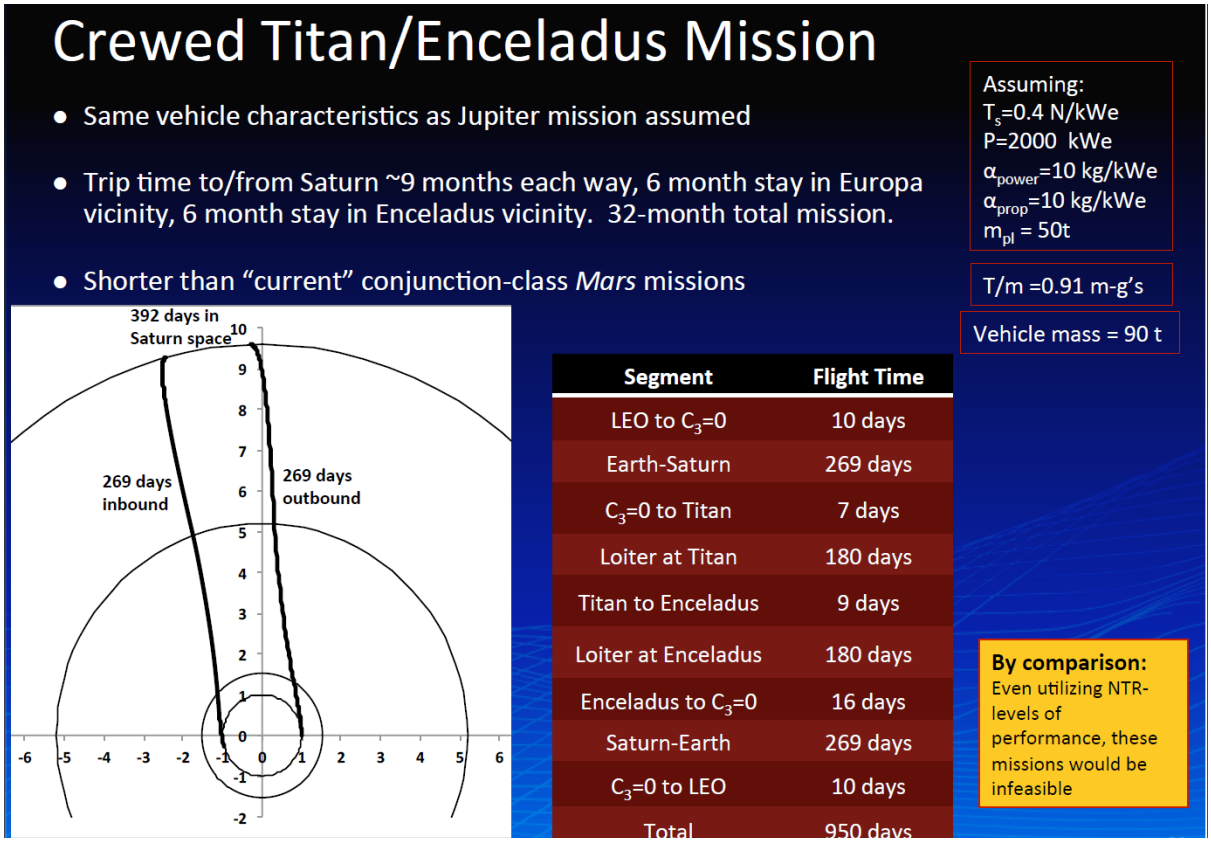

Figure 25. 2MW NEP (90t spacecraft) Crewed Titan/Enceladus Mission with 0.4N/kW$_e$ thrust to power

VI. Summary and Forward Work

This paper describes the methodology used to successfully design and operate a prototype thruster capable of interacting with the fluctuations in the quantum vacuum to a thrust level that is detectable using a low thrust torsion pendulum with a micronewton sensitivity. It briefly describes a previous campaign performed by a highly regarded aerospace engineering university in China that explored a possibly related implementation up to very high power levels. It subsequently has described a formal test campaign conducted recently to evaluate RF resonant cavity thruster performance, including the use of dielectric RF resonators. The recent experiences with the RF thruster implementations has provided some useful lessons learned and new insights on how to improve analysis fidelity and testing protocols. These experiences have directly influenced the follow-on activities that are currently in work and will be briefly highlighted. Moving forward, a new tapered cavity RF resonance system has been designed and characterized using COMSOL® with Q-thruster physics. Figure 26 shows some of the COMSOL® analysis with the higher performance dielectric resonator clearly visible. This resonator material has a relative permittivity that is an order of magnitude higher than our current tapered cavity test article resonator material. The lessons learned with antenna design and location have been factored in and the design of both the drive and sense antennas have been explicitly optimized to excite the RF thruster at the target frequency and mode (e.g., the optimal location has been analytically determined). The thrust performance of this next generation tapered test article has been analytically determined to be in the 0.1 newton per kilowatt regime. Vacuum compatible RF amplifiers with power ranges of up to 125 watts will allow testing at vacuum conditions which was not possible using our current RF amplifiers due to the presence of electrolytic capacitors. The tapered thruster has a mechanical design such that it will be able to hold pressure at 14.7 pounds per square inch (psi) inside of the thruster body while the thruster is tested at vacuum to preclude glow discharge within the thruster body while it is being operated at high power. A phase lock loop (PLL) solution has already been implemented and evaluated at the 1 GHz frequency range, and is being tailored to be able to support testing at multiple set points all the way up to 2.5 GHz. The near term objective is to complete a Q-thruster breadboard test article that is capable of being shipped to other locations which possess the ability to measure low thrust for independent verification and validation (IV&V) of the technology. The current plan is to support an IV&V test campaign at the Glenn Research Center (GRC) using their low thrust torsion pendulum followed by a repeat campaign at the Jet Propulsion Laboratory (JPL) using their low thrust torsion pendulum. The Johns Hopkins University Applied Physics Laboratory has also expressed an interest in performing a Cavendish Balance style test with the IV&V shipset.

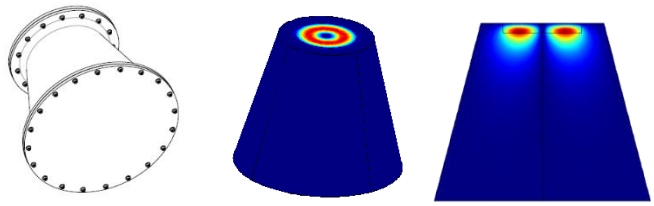

Figure 26. Next Generation RF Thruster

Acknowledgments

D. A. Brady thanks his mentors who, not coincidentally, are the co-authors on this paper. Without their insight, teaching, and patience, he would have been unable to undertake this project. In addition, he thanks Kent Joosten for his substantial contribution to Q-thruster mission analysis.

References

[1] Y. Juan, et. al., Chin. Phys. B **22**, 050301 (2013).
[2] D. Blas, M. M. Ivanov and S. Sibiryakov, JCAP **1210**, 057 (2012) [arXiv:1209.0464 [astro-ph.CO]].
[3] URL: http://cannae.com/ [cited 24 June 2014]